

Bispectral analysis of nonlinear compressional waves in a 2D dusty plasma crystal

V. Nosenko*, J. Goree, and F. Skiff

Department of Physics and Astronomy,

The University of Iowa, Iowa City Iowa 52242

(Dated: August 30, 2005)

Abstract

Bispectral analysis was used to study the nonlinear interaction of compressional waves in a 2D strongly coupled dusty plasma. A monolayer of highly charged polymer microspheres was suspended in a plasma sheath. The microspheres interacted with a Yukawa potential and formed a triangular lattice. Two sinusoidal pump waves with different frequencies were excited in the lattice by pushing the particles with modulated Ar^+ laser beams. Waves at the sum, difference, and other combination frequencies were shown to be the result of coherent nonlinear interaction of pump waves. However, for certain combination frequencies coherent nonlinear interaction was ruled out.

PACS numbers: 52.27.Lw, 82.70.Dd, 52.35.Mw, 52.27.Gr

[1] Electronic mail: vladimir-nosenko@uiowa.edu

I. INTRODUCTION

Bispectral analysis is a powerful tool to study nonlinear phenomena [1]. In this method, a correlation is calculated between fluctuations at different frequencies in Fourier spectra of the waves studied. If the correlation among a triplet of waves at frequencies F_1 , F_2 , and $F_1 + F_2$ is strong, this result indicates phase coupling between these waves. In this case, the wave at $F_1 + F_2$ is a result of coherent nonlinear interaction of waves at F_1 and F_2 . If there is no correlation in the triplet F_1 , F_2 , and $F_1 + F_2$, this rules out the coherent nonlinear interaction of waves at F_1 and F_2 .

In this paper, we use bispectral analysis to clarify questions that remained unresolved in Ref. [2]. In that paper, an experiment was reported where nonlinear three-wave interaction of compressional waves was observed in a 2D dusty plasma.

A dusty plasma is a suspension of micron-size particles in a plasma. The particles are highly charged, and due to mutual repulsion in combination with the natural confinement provided by the plasma's radial electric field, they arrange themselves in a structure, called a plasma crystal, with crystalline or liquid-like order. In the presence of gravity, particles can settle in a 2D monolayer, whereas the plasma's electrons and ions fill a 3D volume. The particles can be imaged directly, and their positions and velocities calculated, which allows studying the lattice microscopically.

Sound waves, or phonons, are well-studied in the linear or low-amplitude limit. The literature, both theoretical and experimental, for 2D dusty plasmas is reviewed in Ref. [3] and references cited therein.

The properties of nonlinear waves in dusty plasmas have also been studied, but not as completely as for linear waves. It was shown theoretically that nonlinear pulses can take the form of solitons in weakly [4] and strongly coupled [5–7] dusty plasmas, although frictional gas damping can suppress soliton formation [6, 7]. In experiments with large amplitudes, nonlinear pulses [5, 8] and harmonic generation [2, 9] were observed in 2D lattices. Harmonic generation was explained theoretically in Refs. [9, 10].

II. REVIEW OF EXPERIMENT

In this paper we will present further analysis, using different methods, of the experiment of Nosenko and Goree [2], where nonlinear mixing of compressional waves was observed in a 2D dusty plasma crystal. Below, we will briefly review the experimental procedure and main results of Ref. [2].

A monolayer of highly charged polymer microspheres was suspended in a plasma sheath, Fig. 1. The particle suspension had a diameter of about 60 mm. The particles had a diameter of $8.09 \pm 0.18 \mu\text{m}$ [11] and a mass density 1.514 g/cm^3 . To achieve a low damping rate, Ar gas was used at a pressure of 5 mTorr, so that the gas drag, which is accurately modeled [11] by the Epstein expression, was only $\nu_d = 0.87 \text{ s}^{-1}$. The plasma was sustained by a 13.56 MHz rf voltage with a peak-to-peak amplitude of 168 V and a self-bias of -115 V .

The particles in the suspension arranged themselves in a triangular lattice, as shown in the image in Fig. 1(a). The interparticle spacing was $a = 675 \pm 14 \mu\text{m}$, as identified by the first peak in the pair correlation function $g(r)$. The lattice was in an ordered state; $g(r)$ had many peaks, and it had translational order length of $16a$ in an undisturbed lattice, although this diminished to $4a$ when large-amplitude waves were excited. A pulse technique [12] making use of a theoretical wave dispersion relation was used to measure the particle charge $Q = -9400 \pm 900e$ and screening length $\lambda_D = 0.73 \pm 0.10 \text{ mm}$ at the particles' height.

The particles were imaged through the top window by a video camera, and they were illuminated by a horizontal He-Ne laser sheet. Movies of 68.3–136.7 s duration were digitized using a digital VCR at 29.97 frames per second. The $24 \times 18 \text{ mm}$ field of view included 1000 – 1100 particles, Fig. 1(a). Particle coordinates and velocities were then calculated in each frame using the moment method [13]. The $x - y$ coordinate system in the plane of particle suspension has its x axis in the direction of the laser beam, as shown in Fig. 1(b), so that waves propagated in the $\pm x$ directions.

A laser-manipulation method was used to excite two sinusoidal compressional pump waves with different frequencies $f_1 = 0.7 \text{ Hz}$, $f_2 = 1.7 \text{ Hz}$ and parallel wave fronts in the plasma crystal, Fig. 1. Particles were pushed by the radiation pressure force, which is proportional to an incident laser intensity [11]. Measurements were repeated with three different laser powers to vary the pump strength, and also with no laser power. We will report the laser power as measured inside the vacuum chamber. Our highest power was 3.41 W. Note

that this power was distributed over a narrow rectangular stripe that traversed the particle suspension. To understand how large the pump power was, the most physically significant parameter is the peak velocity of the particles in the stripe where the laser struck. This peak velocity was 0.72 mm/s, corresponding to 3.3% of the sound speed for compressional waves, at our highest laser power of 3.41 W.

The results of this experiment as reported in Ref. [2] were observation of the waves propagating in the lattice at the sum, difference, and other combination frequencies, as well as harmonics of the pump waves. The waves at the sum frequencies $f_1 + f_2$ and $2f_1 + f_2$ were found to be generated only above an excitation-power threshold. This threshold was attributed to frictional damping, as predicted by nonlinear wave theory [2].

III. ANALYSIS METHOD

In the present paper, we use a different method, bispectral analysis, to clarify the mechanism of generating waves at different combination frequencies in the experiment of Ref. [2]. We performed bispectral analysis of the particle velocity using the following procedure. The x -component of the particle velocity was spatially averaged within 40 rectangular bins elongated along the y axis. The Fourier transform $v_x(f)$ of the averaged particle velocity $v_x(t)$ was then computed for each of the 40 bins. Then we calculated the maps of the squared bicoherence:

$$\gamma^2(F_1, F_2) = \frac{|\langle v_x(F_1) v_x(F_2) v_x^*(F_1 + F_2) \rangle|^2}{\langle |v_x(F_1) v_x(F_2)|^2 \rangle \langle |v_x(F_1 + F_2)|^2 \rangle}, \quad (1)$$

where $\langle \dots \rangle$ denotes the ensemble average and v_x^* is the complex conjugate of v_x . Ensemble averaging was performed in 9 data bins that were located 6.5 – 11.1 mm away from the excitation region. The amplitudes of waves at combination frequencies did not change significantly between these data bins. In addition, the 4096-frame time sequence of $v_x(t)$ in each of these bins was divided into four 1024-frame sub-sequences. Thus we obtained $n = 36$ ensembles, each 1024 frames long, to calculate the ensemble average. The length of each ensemble was enough to calculate $v_x(f)$ with sufficient frequency resolution.

The aim of using bispectral analysis is to determine whether there is significant coupling between three waves, as indicated by a strong correlation. It is customary to characterize the coupling as strong if γ^2 is nearly unity and absent if it is near zero [14]. Coupling that is not strong can nevertheless be deemed statistically significant at the 95% confidence level if

$\gamma^2 > 3/n$, which for our case is $\gamma^2 > 0.083$. We will test three different experimental cases, corresponding to three different pump power levels, and we will find that strong coupling, with γ^2 near unity, occurs in two of these cases, for the experiment of Ref. [2].

IV. RESULTS

A. Compressional waves

Going beyond the power spectra reported in Ref. [2], we also present two other kinds of maps. These are maps of the bicoherence $\gamma^2(F_1, F_2)$ and maps of the wave energy in $\omega-k$ space. The maps of γ^2 are presented as functions of two independent variables, F_1 and F_2 ; these should not be confused with f_1 and f_2 , which represent the two pump frequencies in the experiment. The bicoherence maps indicate whether a coherent nonlinear coupling occurs amongst three oscillations. Whether these oscillations correspond to a propagating wave or some other oscillation such as a sloshing mode is revealed by the energy maps in $\omega-k$ space. The maps of bicoherence and of energy in $\omega-k$ space are new for this paper; they were not previously reported in Ref. [2] for the same experiment.

At our highest amplitude for the pump waves, with a laser power of 3.41 W, the power spectrum of particle velocity has peaks corresponding to the pump waves, their harmonics, and waves at various combination frequencies, as shown in Fig. 2(a). This figure is similar to Fig. 2(a) of Ref. [2], except that in the present paper the power spectrum was calculated in the same region of the plasma crystal located 6.5 – 11.1 mm away from the excitation region that was used to calculate bicoherence. Next, we examine our results for the two other kinds of maps, bicoherence and wave energy in $\omega-k$ space, which are new for this paper.

The map of squared bicoherence γ^2 in Fig. 2(b) shows that the waves at combination frequencies are a result of coherent nonlinear interaction of the pump waves, thus supporting a similar conclusion made in Ref. [2]. The black dots in this map indicate the pairs of frequencies F_1, F_2 , where the squared bicoherence $\gamma^2(F_1, F_2)$ is nearly unity, indicating strong coupling. For any point on the map where γ^2 is near unity, we conclude that the corresponding frequencies F_1, F_2 , and $F_1 + F_2$ are not only harmonically related, but phase coupled as well, which is a signature of coherent nonlinear interaction between the waves at F_1 and F_2 . For example, for the point on the map corresponding to our two pump

frequencies, the value of the squared bicoherence is near unity, $\gamma^2(f_1, f_2) = 0.954$. This peak shows that a third wave exists with a frequency $f_1 + f_2 = 2.4$ Hz, and that the phase of this wave equals $\phi_1 + \phi_2$, where ϕ_1 and ϕ_2 are the phases of the waves at f_1 and f_2 . For this example, one can conclude that the generation mechanism for the sum-frequency wave is coherent nonlinear interaction of the pump waves.

We will now compare the map of squared bicoherence γ^2 in Fig. 2(b) and the power spectrum $|v_x(f)|^2$ for particle motion in Fig. 2(a). Each peak at a combination frequency in the power spectrum in Fig. 2(a) has one or more corresponding peaks in the bicoherence map in Fig. 2(b). The latter peaks show different ways the wave at that combination frequency was generated. There is one exception, though. For the peak at $2f_1 + 2f_2 = 4.8$ Hz in Fig. 2(a), there is no corresponding peak in Fig. 2(b). We will discuss the significance of this finding for the wave at 4.8 Hz later in this paper.

At our medium amplitude for the pump waves, with a laser power of 1.19 W, the power spectrum of particle velocity has fewer peaks, in Fig. 3(a). Some combination-frequency peaks have disappeared at this lower amplitude, as compared to the higher amplitude case of Fig. 2. This occurs because the pump amplitude became lower than the threshold value, as explained by the theory of Ref. [2]. Remaining peaks at the combination frequencies of $f_2 - f_1$, $f_1 + f_2$, and $2f_1 + f_2$ are still a result of coherent nonlinear interaction of the pump waves, as indicated by corresponding peaks in the map of bicoherence in Fig. 3(b), where γ^2 is near unity. For example, at the point corresponding to our two pump frequencies, the squared bicoherence is $\gamma^2(f_1, f_2) = 0.957$.

At our lowest amplitude of the pump waves, with a laser power of 0.11 W, the power spectrum of particle velocity in Fig. 4(a) has, besides the pump frequencies, two peaks at the combination frequencies $f_2 - f_1 = 1.0$ Hz and $2f_1 + 2f_2 = 4.8$ Hz, and lower peaks at frequencies that seem to be unrelated to the pump frequencies. However, there are no peaks with γ^2 near unity in the corresponding map of bicoherence in Fig. 4(b). For example, at the point corresponding to our two pump frequencies, the squared bicoherence is $\gamma^2(f_1, f_2) = 0.022$. This means that there is no coherent nonlinear interaction of the pump waves when they have low amplitude, in agreement with the theory of Ref. [2]. The origin of the peaks at 1.0 Hz and 4.8 Hz in Fig. 4(a) thus remains unclear. We will discuss the waves at 1.0 Hz and 4.8 Hz later in this paper.

The chief result of this paper is that using bispectral analysis verifies the theoretical

prediction of Ref. [2] of an excitation-power threshold for the generation of a difference-frequency wave. The peak at the difference frequency $f_2 - f_1 = 1.0$ Hz is present in the power spectra of the particle velocity at all values of laser power, as shown in Figs. 2(a), 3(a), 4(a). However, the corresponding peaks in the respective maps of bicoherence are only present at the two higher values of laser power, Figs. 2(b) and 3(b). Compare, for example, Figs. 3 and 4. The peak at 1.0 Hz is present in the power spectra in Figs. 3(a) and 4(a), with similar amplitudes, yet the corresponding peak in the map of bicoherence is only present in Fig. 3(b). In general, the peak at 1.0 Hz is present in the maps of bicoherence at laser powers of 1.19 W and higher, while it is missing at laser powers of 0.61 W and below. This means that the wave at $f_2 - f_1 = 1.0$ Hz is phase coupled to the pump waves for $P_{\text{laser}} \geq 1.19$ W, but it is not phase coupled to the pump waves for $P_{\text{laser}} \leq 0.61$ W. Hence the wave at 1.0 Hz can be attributed to coherent nonlinear mixing of the pump waves only at higher values of laser power $P_{\text{laser}} \geq 1.19$ W, in agreement with the prediction of theory of Ref. [2] that there is an excitation-power threshold for generation of combination-frequency waves.

Similarly, bispectral analysis helps to reveal that the peak at 4.8 Hz in the power spectra of the particle velocity is not a result of coherent nonlinear mixing of the pump waves regardless of their amplitude, even though this peak happens to be at the combination frequency $2f_1 + 2f_2$. Indeed, the phase of the wave at 4.8 Hz is not coupled to the phases of the pump waves, as evidenced by the absence of the corresponding peaks in the maps of bicoherence in Figs. 2(b), 4(b).

B. Other oscillations

While bispectral analysis can tell us that the waves at $f_2 - f_1 = 1.0$ Hz (below the excitation-power threshold) and $2f_1 + 2f_2 = 4.8$ Hz *are not* a result of coherent nonlinear mixing of the pump waves, it cannot tell us what they *are*. In particular, it cannot tell us whether the observed oscillations are propagating waves. For that purpose, we need an additional method, described next.

A more complete identification of observed oscillations can be obtained from the analysis of the map of wave energy in ω - k space shown in Fig. 5. The wave energy is mostly concentrated in distinct peaks that correspond to the pump waves, their harmonics, and waves at combination frequencies. These peaks are superimposed on weaker curved stripes represent-

ing the dispersion relation of spontaneously excited compressional waves, as observed in the experiment in Ref. [16]. However, some peaks in Fig. 5 do not lie on the dispersion relation. Most notably, the oscillations at 4.8 Hz and 6.3 Hz have a wave number $k \approx 0$. These are therefore close to a sloshing mode, i.e., a motion of all particles together as a rigid body in the confining potential provided by the plasma's radial electric field [17]. Such an oscillation does not satisfy the compressional wave's dispersion relation. This observation supports the conclusion made earlier that the oscillation at 4.8 Hz is not generated by coherent nonlinear mixing of the pump waves. Therefore, it is only a coincidence that this oscillation happens to be at the combination frequency $2f_1 + 2f_2 = 4.8$ Hz. It may be excited by a spontaneous motion of a lattice defect or an energetic particle beneath the monolayer [18]. It may also be an artifact due to camera vibration or noise in the camera and electronics. This oscillation at 4.8 Hz might indeed be intermittent, because it is absent for the data series presented in Fig. 3.

Similarly, the oscillation at 1.0 Hz has a wave number $k \approx 0$ at our lowest amplitude, which is below the excitation-power threshold, Fig. 5(b). This means that below the excitation-power threshold, this oscillation, as in the case of 4.8 Hz, is a long-wavelength motion of particles probably caused by oscillating defects or particles beneath the monolayer. On the other hand, above the excitation-power threshold, the wave at 1.0 Hz has a finite wave number $k \neq 0$, that lies on the dispersion relation of compressional waves, as shown in Fig. 5(a). This supports the conclusion that the difference-frequency wave is generated by coherent nonlinear mixing of the pump waves, above the excitation-power threshold.

Finally, we note some faint unexplained features in the map of bicoherence for the lowest pump amplitude, Fig. 4(b). Even though there is no coherent nonlinear interaction of the pump waves when they have low amplitudes, the map of bicoherence in Fig. 4(b) has peaks at random frequencies in the range $F_{1,2} \leq 1$ Hz. These peaks are weak, with a squared bicoherence of only $\gamma^2 \leq 0.4$. The frequencies of these random peaks, however, are unrelated to the pump frequencies. Similar peaks with $\gamma^2 \leq 0.3$ are present even without any external excitation (zero pump amplitude). These bicoherence levels indicate that the coupling is not strong, although they might be statistically significant. The latter observation might be an indication of phase coupling between spontaneously excited low-frequency long-wavelength waves in a 2D plasma crystal. On the other hand, these features at low amplitude might also be merely artifacts of the random errors in our velocity measurements.

V. USES OF BISPECTRAL ANALYSIS BEYOND BICOHERENCE

Bispectral analysis can provide more information on nonlinear wave interaction than is illustrated in this paper. Rather than use the bicoherence γ^2 , one could use the bispectrum

$$B(F_1, F_2) = \langle v_x(F_1) v_x(F_2) v_x^*(F_1 + F_2) \rangle, \quad (2)$$

where we have used the same notations as in Eq. 1. It can be shown that the imaginary part of the bispectrum carries information on the rate of power transfer between different modes. This method will be described in detail elsewhere.

VI. ACKNOWLEDGMENTS

This work was supported by NASA and U.S. Department of Energy.

-
- [1] T. Subba Rao and M.M. Gabr, *Lecture Notes in Statistics. An Introduction to Bispectral Analysis and Bilinear Time Series Models* (Springer-Verlag, New York Berlin Heidelberg Tokyo, 1984), Vol. 24.
 - [2] V. Nosenko, K. Avinash, J. Goree, and B. Liu, *Phys. Rev. Lett.* **92**, 085001 (2004).
 - [3] A. Piel *et al.*, *J. Phys. B* **36**, 533 (2003).
 - [4] N.N. Rao, P.K. Shukla, and M.Y. Yu, *Planet. Space Sci.* **38**, 543 (1990).
 - [5] D. Samsonov *et al.*, *Phys. Rev. Lett.* **88**, 095004 (2002).
 - [6] S. Zhdanov, D. Samsonov, and G. Morfill, *Phys. Rev. E* **66**, 026411 (2002).
 - [7] K. Avinash *et al.*, *Phys. Rev. E* **68**, 046402 (2003).
 - [8] V. Nosenko, S. Nunomura, and J. Goree, *Phys. Rev. Lett.* **88**, 215002 (2002).
 - [9] S. Nunomura *et al.*, *Phys. Rev. E* **68**, 026407 (2003).
 - [10] K. Avinash *et al.*, *Phys. Plasmas* **11**, 1891 (2004).
 - [11] B. Liu *et al.*, *Phys. Plasmas* **10**, 9 (2003).
 - [12] V. Nosenko, J. Goree, Z.W. Ma, and A. Piel, *Phys. Rev. Lett.* **88**, 135001 (2002).
 - [13] A. Melzer *et al.*, *Phys. Rev. E* **62**, 4162 (2000).
 - [14] K. Kim and S. Kim, *J. Phys. Soc. Jpn.* **65**, 2323 (1996).
 - [15] R.A. Haubrich, *J. Geophys. Res.* **70**, 1415 (1965).

FIG. 1: Experimental apparatus. (a) Particles arranged in a triangular 2D lattice. Atop this image is a sketch showing where the radiation pressure force from two modulated Ar⁺ laser sheets pushes particles, exciting sinusoidal compressional pump waves. (b) The particles are polymer microspheres, suspended as a monolayer above the lower electrode in a capacitively coupled rf plasma. All our analysis is based on images recorded by the top-view camera.

FIG. 2: (a) Power spectrum $|v_x(f)|^2$ and (b) map of the squared bicoherence $\gamma^2(F_1, F_2)$ of the particle velocity. Note that f , F_1 , and F_2 denote independent variables, whereas $f_1 = 0.7$ Hz and $f_2 = 1.7$ Hz are the pump frequencies. Data shown here are for a high excitation laser power of 3.41 W. Black dots in (b) indicate the pairs of frequencies F_1 , F_2 , where bicoherence is high, $\gamma^2(F_1, F_2) \approx 1$. The waves with corresponding frequencies F_1 , F_2 , and $F_1 + F_2$ are not only harmonically related, but phase coupled as well, which is a signature of coherent nonlinear interaction between the waves at F_1 and F_2 . For example, the points at (f_1, f_2) and (f_2, f_1) represent the generation of the combination frequency $f_1 + f_2$, where f_1 and f_2 are the pump frequencies.

[16] S. Nunomura *et al.*, Phys. Rev. Lett. **89**, 035001 (2002).

[17] S. Nunomura *et al.*, Phys. Rev. E **65**, 066402 (2002).

[18] V.A. Schweigert, I.V. Schweigert, V. Nosenko, J. Goree, Phys. Plasmas **9**, 4465 (2002).

FIG. 3: (a) Power spectrum $|v_x(f)|^2$ and (b) map of the squared bicoherence $\gamma^2(F_1, F_2)$ of the particle velocity for the medium excitation laser power of 1.19 W. The waves at combination frequencies $f_2 - f_1$, $f_2 + f_1$, and $2f_1 + f_2$ are generated by coherent nonlinear mixing of the pump waves, as indicated by corresponding peaks in bicoherence, where $\gamma^2 \approx 1$.

FIG. 4: (a) Power spectrum $|v_x(f)|^2$ and (b) map of the squared bicoherence $\gamma^2(F_1, F_2)$ of the particle velocity for the low excitation laser power of 0.11 W. The power spectrum has peaks at combination frequencies $f_2 - f_1 = 1.0$ Hz and $2f_1 + 2f_2 = 4.8$ Hz. However, bicoherence $\gamma^2 \ll 1$ for all frequencies. This rules out coherent nonlinear interaction of the pump waves at this low amplitude.

FIG. 5: Map of wave energy in ω - k space for (a) high and (b) low excitation laser power. The levels of laser power in (a) and (b) correspond to Figs. 2 and 4, respectively. The wave energy is mostly concentrated in distinct peaks that correspond to the pump waves, their harmonics, and waves at combination frequencies. These peaks are superimposed on weaker stripes representing the dispersion relation of spontaneously excited compressional waves [16]. The oscillation at 4.8 Hz has a wave number $k \approx 0$ and does not satisfy the dispersion relation. This oscillation is not generated by coherent nonlinear interaction of the pump waves, even though it happens to be at the frequency $2f_1 + 2f_2 = 4.8$ Hz.

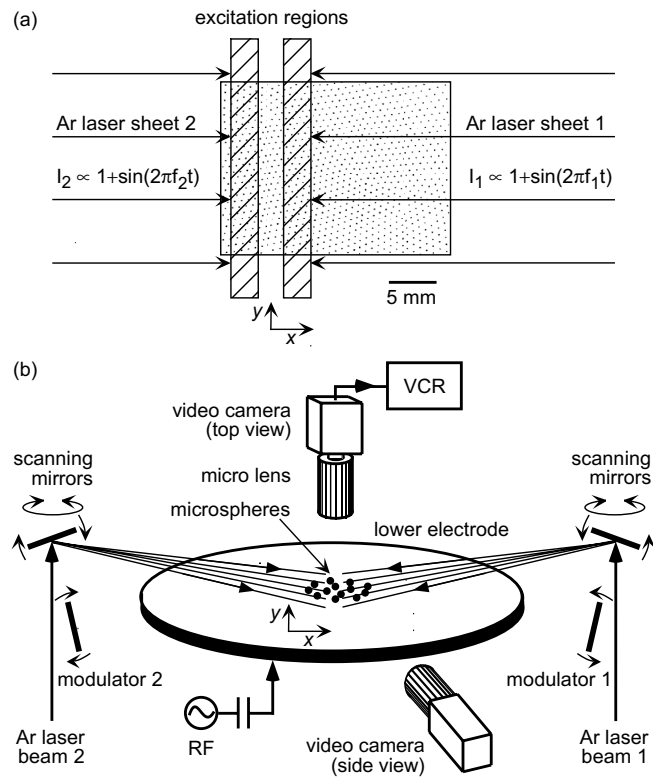


Fig. 1

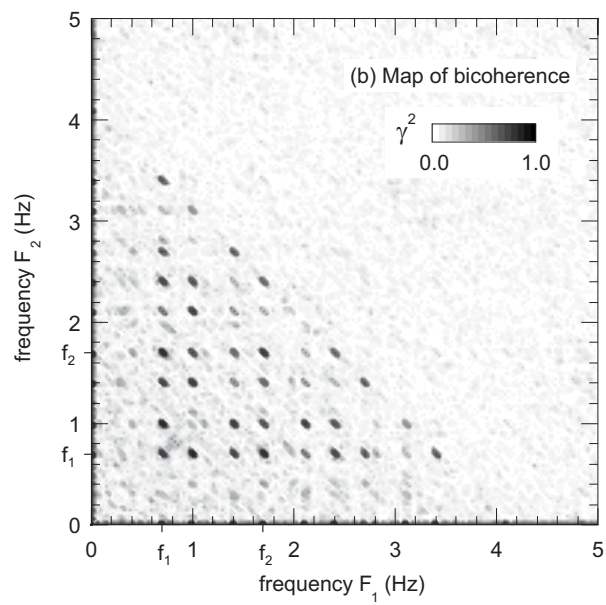
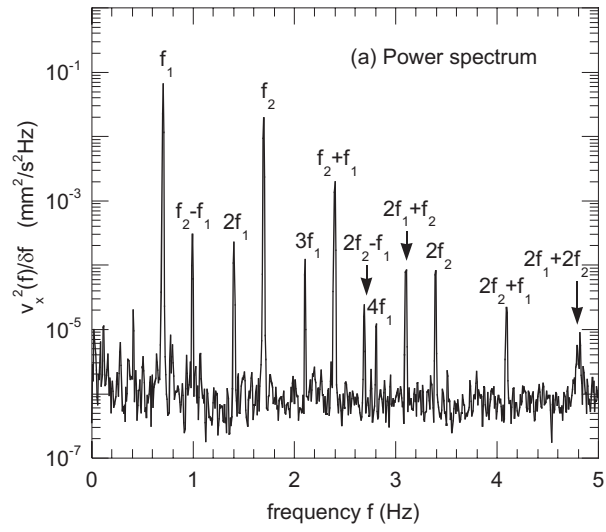


Fig. 2

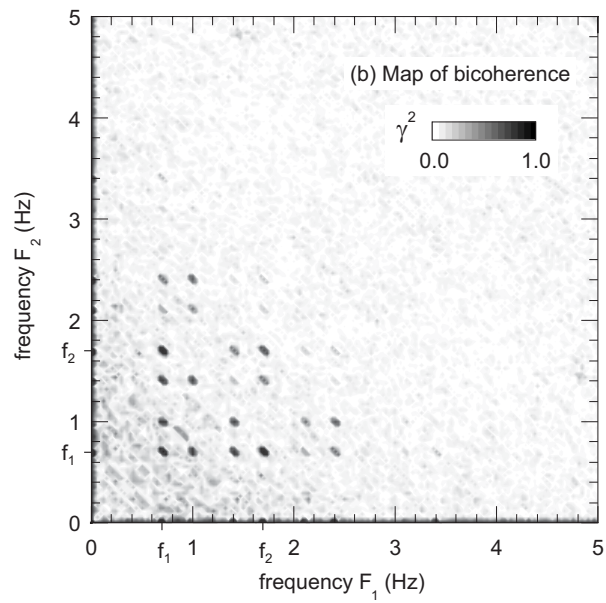
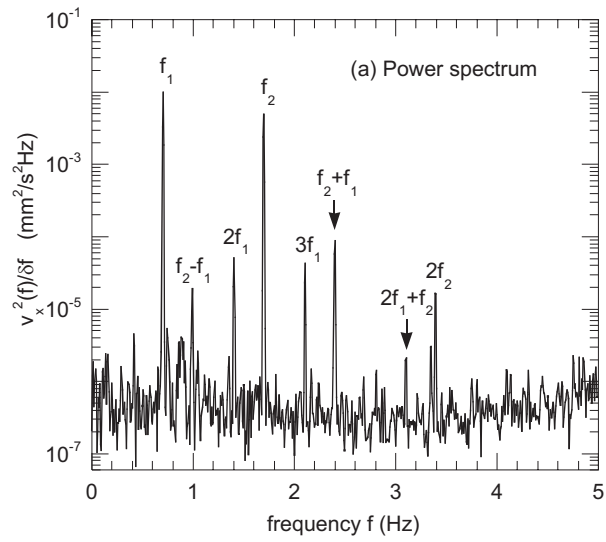


Fig. 3

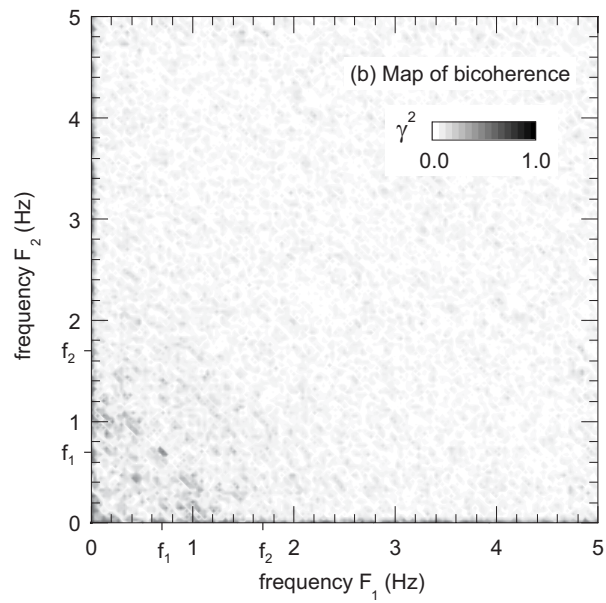
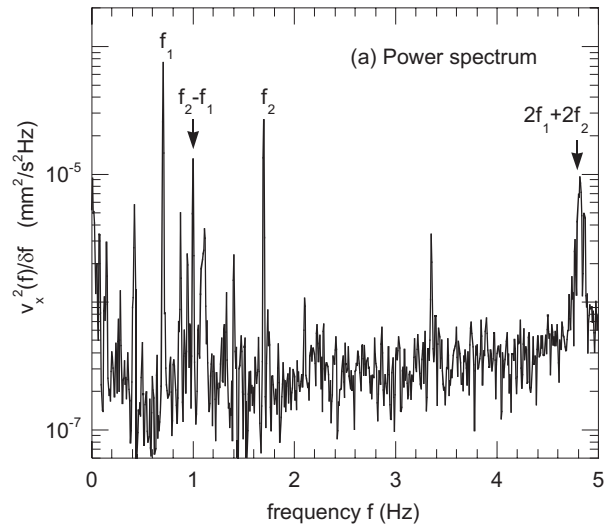


Fig. 4

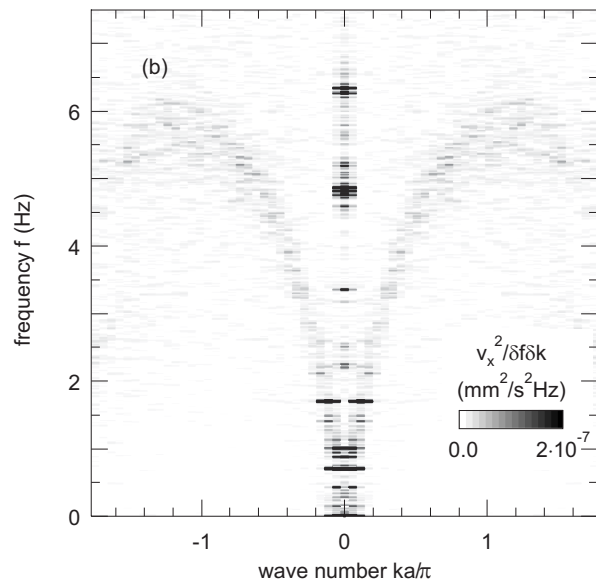
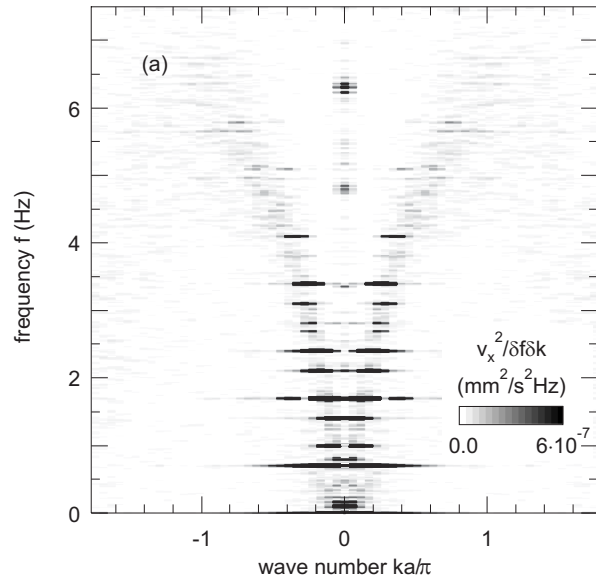


Fig. 5